IEICE TRANS. INF. & SYST., VOL.E79-D, NO.4 APRIL 1996

PAPER

Compensation for the Distortion of Bipolar Surface EMG Signals Caused by Innervation Zone Movement

Hidekazu KANEKO†, Tohru KIRYU††, *and* Yoshiaki SAITOH††, *Members*

SUMMARY A novel method of multichannel surface EMG processing has been developed to compensate for the distortion in bipolar surface EMG signals due to the movement of innervation zones. The distortion of bipolar surface EMG signals was mathematically described as a filtering function. A compensating technique for such distorted bipolar surface EMG signals was developed for the brachial biceps during dynamic contractions in which the muscle length and tension change. The technique is based on multichannel surface EMG measurement, a method for estimating the movement of an innervation zone, and the inverse filtering technique. As a result, the distorted EMG signals were compensated and transformed into nearly identical waveforms, independent of the movement of the innervation zone.

key words: *innervation zone, conduction velocity, multichannel EMG, inverse filtering, brachial biceps*

1. Introduction

Depending on the electrode configuration, bipolar surface electromyographic (EMG) signals are significantly affected by the filtering effects of the intervening tissue and the spatial filters concerned with bipolar arrangement [1], [2]. In particular, the characteristics of the spatial filtering effects are changed by the movement of innervation zones relative to the recording electrodes. An innervation zone is a narrow band running across muscle fibers in which myoneural junctions are distributed. Recently, Masuda and Sadoyama[3] reported the distribution of several innervation zones in brachial biceps. Some researchers have studied the influence of the position of innervation zones on the EMG signals [4], [5], and reported that the frequency indices of EMG signals were maximum near the neuromuscular junctions. During dynamic contractions in which the muscle length and tension change, the EMG signals are changed not only by the muscle activity but also by the shift of the innervation zones relative to the surface electrodes. This is a serious issue that must be resolved to enable the evaluation of the EMG signals.

The conventional approaches dealing with the influence of the position of innervation zones were indirect solutions. For example, it is common to locate electrodes away from innervation zones to minimize their effects on the recorded signals. However, the innervation zones and their movement must be investigated before actual experiments are conducted in order to properly locate the surface electrodes. Even after the investigation, it is sometimes difficult to properly locate the surface electrodes so as to avoid innervation zones. Our goal was therefore to develop an alternative approach to compensate bipolar surface EMG signals distorted by the innervation zone movement.

Lindström and Magnusson [1] expressed the influence of electrode configuration in terms of filter functions and discussed the influence of physiological parameters including the muscle fiber radius, the conduction velocity of action potentials, and the depth of myofibers below the skin surface. According to their paper, the bipolar electrode configuration produces dips in the spectrum which are related to the conduction velocity and the electrode distance. From the latter half of the 1980s, the importance of the electrode configuration was recognized in surface EMG measurement. Reucher et al. [2] revealed a suitable spatial filter design by comparing several types of electrode configurations. However, a mathematical representation of the filter function related to the movement of innervation zones remains to be developed. A technique to estimate the position of innervation zones was proposed by Masuda and Sadoyama in 1988 [6], which used a spatial representation of action potentials as a function of time. Due to the complicated propagation pattern during dynamic contractions, it was mainly applicable only during isometric contractions. To consider the effects of the movement of innervation zones on surface EMG measurements, it is necessary to estimate the position of the innervation zones even during dynamic contractions.

In this paper, a method that can compensate distorted EMG signals by using an inverse filtering method is described. First, to clarify the influence of the movement of an innervation zone, a mathematical model for the propagation of the action potentials is proposed. Second, an alternative technique for estimating the location of the innervation zone during dynamic contractions is developed. The technique is based on the multichannel surface EMG measurement and instantaneous correlation. Finally, the inverse filtering function derived from the model is applied to compensate the distorted surface EMG signals.

Manuscript received September 11, 1995.

† The author is with National Institute of Bioscience and Human-Technology, AIST, MITI, Tsukuba-shi, 305 Japan.

†† The authors are with the Faculty of Engineering, Niigata University, Niigata-shi, 950-21 Japan.

2. Method

2.1 Propagation Model of Action Potentials

A surface electrode may detect the activity of many myofibers from different motor units. Since the endplates are randomly distributed in the zone of innervation, the influence of the position of the innervation zone on surface EMG signals is not simple. Masuda and Sadoyama [3] studied innervation zones in brachial biceps and found them to be located in the middle of the muscles. Furthermore, their results imply that the possibility of the activation of two or more motor units at the same time is reduced during weak muscle contractions. For simplicity, assume that the action potentials of two or more motor units are not produced at the same time and that the endplates of a motor unit are not distributed over a wide range, but are concentrated in a line across the myofibers. Moreover, assume that the propagation of the action potentials on myofibers abides by concepts such as double conduction (conducting to both directions), decrementless conduction (conducting without any distortion), and isolated conduction (conducting without rendering other other myofibers active), and finally, assume that the action potentials on any myofibers propagate with a constant velocity.

The propagation model of action potentials shown in Fig. 1(a) can be applied, where the electrodes x_k (for $k = 0$ to N) are pasted on the skin along the axis of conduction of the myofibers (i.e., along the X-axis) at the same interval δ. The parameter $x_{(t)}$ is the average position of the endplates innervated by a motor neuron at time t. In this model, the action potential $g_{(t)}$ is generated at $x_{(t)}$ by the excitation of the motor neuron, and propagates in both directions along the X-axis with the conduction velocity $v_{(t)}$. The spatial distribution of the action potential is represented by

$$f_{(t,x)} = g\left(t - \frac{|x - x_{(t)}|}{v_{(t)}}\right). \tag{1}$$

Here, t is time and x is position. $f_{(t,x)}$ is symmetrical with $x_{(t)}$, because $f_{(t,x_{(t)}+x)} = f_{(t,x_{(t)}-x)}$.

Using multichannel surface electrodes, we can obtain a differential output $s_{i(t)}$ with the bipolar configuration of the i th electrode pair, x_{i-1} and x_i, using

$$s_{i(t)} = f_{(t,x_{i-1})} - f_{(t,x_i)}. \tag{2}$$

The transfer function from $g_{(t)}$ to $s_{i(t)}$ is also described as

$$H_{i(\omega;t)} = \frac{S_{i(\omega;t)}}{G_{i(\omega;t)}} = e^{-j\omega\frac{|x_{i-1}-x_{(t)}|}{v_{(t)}}} - e^{-j\omega\frac{|x_i-x_{(t)}|}{v_{(t)}}}. \tag{3}$$

Here, ω denotes angular frequency. $S_{i(\omega;t)}$ and $G_{i(\omega;t)}$ are the Fourier transforms of $s_{i(t)}$ and $g_{(t)}$, respectively.

The gain and phase characteristics of $H_{i(\omega;t)}$ are expressed using two spatial distances, i.e., the differential interval in (2) and the average distance between $x_{(t)}$ and each electrode pair. The differential interval in (2) corresponds to the spatial distance represented as

$$Dd_{i(t)} = \left||x_{i-1} - x_{(t)}| - |x_i - x_{(t)}|\right|. \tag{4a}$$

The average distance between $x_{(t)}$ and each electrode pair is described as

$$Dm_{i(t)} = \frac{|x_{i-1} - x_{(t)}| + |x_i - x_{(t)}|}{2}. \tag{4b}$$

Both distances are time-variant during the contraction due to muscle movement. When $x_{(t)}$ is not found between the i th electrode pair (i.e., $x_{(t)} < x_i$ or $x_{i-1} < x_{(t)}$), $Dd_{i(t)}$ is equal to the actual geometrical distance δ, and $Dm_{i(t)}$ is longer than $\delta/2$. If $x_{(t)}$ is found between the i th electrode

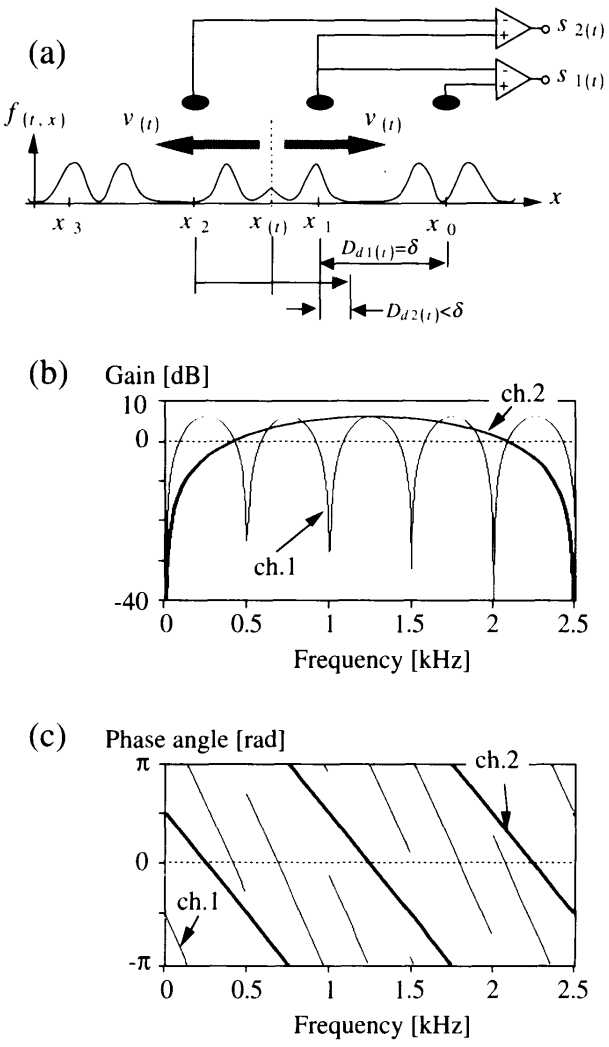

Fig. 1 Propagation model for action potentials. (a) The action potentials derived at $x_{(t)}$ propagate in both directions with the conduction velocity $v_{(t)}$, where concepts such as double conduction, decrementless conduction, and isolated conduction are followed. (b) The gain characteristics of $H_{i(\omega;t)}$ are compared between ch. 1 and ch. 2. The dips of ch. 2 are higher than those of ch. 1. (c). The phase characteristics of $H_{i(\omega;t)}$ are compared between ch. 1 and ch. 2. When the dips appear, the gaps can be seen in the phase angle. In (b) and (c), $D_{1(t)} = 1$ cm $= \delta$, $D_{2(t)} = 0.3$ cm $< \delta$, and $v_{(t)} = 5$ m/s.

pair (i.e., $x_i < x_{(t)} < x_{i-1}$), $Dd_{i(t)}$ is shorter than δ, and $Dm_{i(t)}$ is equal to $\delta/2$.

By using $Dd_{i(t)}$, the gain characteristics of $H_{i(\omega;t)}$ are expressed by

$$|H_{i(\omega;t)}|^2 = 2\left(1 - \cos\frac{\omega Dd_{i(t)}}{v_{(t)}}\right). \quad (5a)$$

On the other hand, by using $Dm_{i(t)}$, the phase characteristics of $H_{i(\omega;t)}$ are expressed as

$$\tan^{-1}\left(\frac{\mathrm{Im}(H_{i(\omega;t)})}{\mathrm{Re}(H_{i(\omega;t)})}\right) = \tan^{-1}\left(\cot\left(\frac{\omega Dm_{i(t)}}{v_{(t)}}\right)\right). \quad (5b)$$

For example, when $Dd_{1(t)}$ and $Dd_{2(t)}$ are, respectively, δ and less than δ as shown in Fig. 1(a), the gain characteristics of $H_{1(\omega;t)}$ and $H_{2(\omega;t)}$ and their phase characteristics are as indicated in Figs. 1(b) and (c), respectively. As shown in Fig. 1(b), the second-lowest frequency dip in $H_{2(\omega;t)}$ is higher than that in $H_{1(\omega;t)}$ because $Dd_{2(t)} < Dd_{1(t)}$. As shown in Fig. 1(c), the phase angles of $H_{1(\omega;t)}$ and $H_{2(\omega;t)}$ do not shift linearly. Since $H_{1(\omega;t)}$ and $H_{2(\omega;t)}$ are nonlinear phase filters, the observed EMG signals are affected by not only the time shift but also the distortion of their waveforms.

Although Lindström and Magnusson [1] and Reucher et al. [2] represented the transfer function of the differential filter as (5a), they did not take into account the movement of the innervation zone. In (5a) and (5b), the movement is clearly displayed by the time variance of $H_{i(\omega;t)}$.

2.2 Estimation of the Average Position of the Endplates innervated by an Active Motor Neuron

To estimate $x_{(t)}$, we measured the surface EMG signals using a multichannel electrode and derived the time delay from each pair of EMG signals. Then the simultaneous equations related to $x_{(t)}$ and $v_{(t)}$ were derived and solved based on the relationship among the conduction velocity, the transition distance, and the time delay.

To derive the time delay, the correlation is calculated from each pair of EMG signals. In dealing with dynamic contractions, we used the natural observation method (NOM) which is an instantaneous signal analysis method developed by Iijima [7]. NOM is used to translate the signal at time t to an instantaneous vector representing its status at t. Figure 2 indicates that the NOM filter transforms $s_{i(t)}$ to the instantaneous vector. The NOM filter consists of cascade filters; a first-order low-pass filter P and M first-order high-pass filters Q_i (for $i = 1$ to M) with the same time constant τ. The observed EMG waveform $s_{i(t)}$ is filtered by the NOM filter and represented by the instantaneous vector in

$$\boldsymbol{S}_{i(t)} = (s_{i,0(t)}, s_{i,1(t)}, s_{i,2(t)}, \ldots, s_{i,M(t)}). \quad (6)$$

M is set such that $s_{i,M(t)}$ is below the background noise level, and τ is set such that the short-time power spectrum of the EMG signal does not change during the period τ. The instantaneous correlation between $\boldsymbol{S}_{i(t)}$ and $\boldsymbol{S}_{j(t)}$ is defined by

$$R_{i,j(T;t)} = \frac{(\boldsymbol{S}_{i(t+T)}, \boldsymbol{S}_{j(t)})}{|\boldsymbol{S}_{i(t+T)}|\,|\boldsymbol{S}_{j(t)}|}. \quad (7)$$

Here $(\cdot,\cdot)$ denotes the inner product and T indicates a time delay of $s_{i(t)}$ relative to $s_{j(t)}$. We set $T^{+}_{i,j(t)}$ as the time delay T which maximizes $R_{i,j(T;t)}$ at time t. In the same way, $T^{-}_{i,j(t)}$ is also set as the time delay T for $s_{i(t)}$ relative to $-s_{j(t)}$.

The simultaneous equations related to $x_{(t)}$ and $v_{(t)}$ are based on the relationships among the conduction velocity, the transition distance, and the time delay. Next, consider the situation in which $x_{(t)}$ is in the range (d_{k+1}, d_k], where d_k denotes the center of the k th bipolar electrode pair (x_{k-1} and x_k). For the i th and j th EMG signals, one of the following equations is used:

$$2x_{(t)} + T^{-}_{i,j(t)} v_{(t)} = d_i + d_j \quad (\text{if } d_j \le d_{k+1} < d_k \le d_i), \quad (8a)$$

$$T^{+}_{i,j(t)} v_{(t)} = d_j - d_i \quad (\text{if } d_j < d_i \le d_{k+1} < d_k), \quad (8b)$$

$$T^{+}_{i,j(t)} v_{(t)} = d_i - d_j \quad (\text{if } d_{k+1} < d_k \le d_j < d_i). \quad (8c)$$

Combining i and j yields the $N(N-1)/2$ equations. Then these simultaneous equations can be solved by the generalized least-squares method.

Here, if $R_{i,j(T^{+}_{i,j(t)};t)}$ or $R_{i,j(T^{-}_{i,j(t)};t)}$ is small, the estimated value of $T^{+}_{i,j(t)}$ or $T^{-}_{i,j(t)}$ is not reliable, respectively. Since unreliable values of $T^{+}_{i,j(t)}$ or $T^{-}_{i,j(t)}$ cause unreliable equations, these simultaneous equations must be solved by the generalized weighted least-squares method to decrease the contribution of the unreliable equations. Thus, each equation is weighted by $R_{i,j(T^{+}_{i,j(t)};t)}$ or $R_{i,j(T^{-}_{i,j(t)};t)}$ as follows:

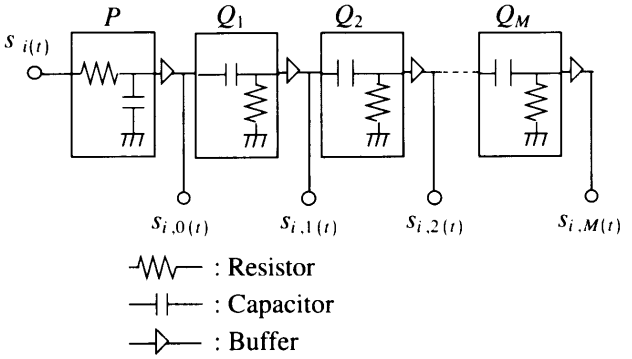

Fig. 2 NOM filter. P is a first-order low-pass filter and Q_i (for $i = 1$ to M) is a first-order high-pass filter. The instantaneous vector of $s_{i(t)}$ has the outputs of these filters as its elements.

$$R_{i,j(T_{i,j(t)};t)}\left(2x_{(t)}+T^{-}_{i,j(t)}v_{(t)}\right)$$
$$=R_{i,j(T_{i,j(t)};t)}(d_i+d_j)$$
$$(\text{if } d_j \le d_{k+1} < d_k \le d_i), \quad (9a)$$

$$R_{i,j(T^{+}_{i,j(t)};t)}\left(T^{+}_{i,j(t)}v_{(t)}\right)=R_{i,j(T^{+}_{i,j(t)};t)}(d_j-d_i)$$
$$(\text{if } d_j < d_i \le d_{k+1} < d_k), \quad (9b)$$

$$R_{i,j(T^{+}_{i,j(t)};t)}\left(T^{+}_{i,j(t)}v_{(t)}\right)=R_{i,j(T^{+}_{i,j(t)};t)}(d_i-d_j)$$
$$(\text{if } d_{k+1} < d_k \le d_j < d_i). \quad (9c)$$

In the generalized weighted least-squares method, the same weighting value is applied both sides of an equation. However it looks like ineffective, when the number of the simultaneous equations is larger than that of variables, the solutions are mainly determined by reliable equations, i.e., heavily weighted equations.

The solution of the simultaneous equations is tested by the assumption that $x_{(t)}$ is in the range (d_{k+1}, d_k), and furthermore by the condition of whether $v_{(t)}$ is reasonable or not (i.e., $\bar{v}-\gamma/2 \le v_{(t)} < \bar{v}+\gamma/2$ or other conditions, where $\bar{v}$ and γ are the mean value and the acceptable range of the conduction velocity, respectively). Finally the positions of the endplates are derived and the position of the innervation zone, $\overline{x_{(t)}}$, is calculated using the estimated local mean value of $x_{(t)}$.

2.3 Compensation Procedure

To compensate for the distortion of the EMG signals caused by the movement of the innervation zone, the inverse filtering method is applied. Assume that the position of the innervation zone and the conduction velocity of action potentials for all myofibers can be approximated by $\overline{x_{(t)}}$ and $\bar{v}$, respectively. The inverse filtering function can be derived as follows.

Using $\overline{x_{(t)}}$ and $\bar{v}$ to (3), the Fourier transform of $s_{i(t)}$ is represented by

$$S_{i(\omega;t)}=\left(e^{-j\omega\frac{|x_{i-1}-\overline{x_{(t)}}|}{\bar{v}}}-e^{-j\omega\frac{|x_i-\overline{x_{(t)}}|}{\bar{v}}}\right)G_{(\omega)}. \quad (10)$$

In (10), $S_{i(\omega;t)}$ is affected by $\overline{x_{(t)}}$, i.e., the movement of the innervation zone. To reduce the interference, we consider the situation where the surface EMG measurement is carried out using electrodes that slide on the skin surface, as shown in Fig. 3. Because the surface electrodes slide synchronously with $\overline{x_{(t)}}$, the positive surface electrode is always located on $\overline{x_{(t)}}$. Here, $Dd_{i(t)}$ and $Dm_{i(t)}$ can be assumed to have constant values of δ and $\delta/2$ respectively. Thus, we refer to the surface EMG signal detected under these conditions as the standard surface EMG signal $c_{(t)}$. The Fourier explanation of $c_{(t)}$ is represented by

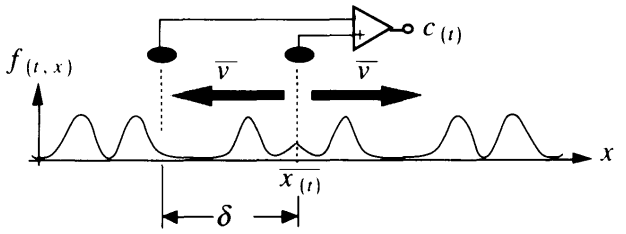

Fig. 3 Standard EMG signals using sliding electrodes. The surface electrodes slide synchronously with $\overline{x_{(t)}}$, and the positive surface electrode is always located on $\overline{x_{(t)}}$. Consequently, $Dd_{i(t)}$ can be assumed to have a constant value of δ.

$$C_{(\omega)}=\left(1-e^{-j\omega\frac{\delta}{\bar{v}}}\right)G_{(\omega)} \quad (11)$$

Using (10) and (11), we can use the inverse filter to obtain $c_{(t)}$ from $s_{i(t)}$. The standard EMG signal calculated from the i th EMG signal $s_{i(t)}$ is given by

$$C_{i(\omega)}=\frac{1-e^{-j\omega\frac{\delta}{\bar{v}}}}{e^{-j\omega\frac{|x_{i-1}-\overline{x_{(t)}}|}{\bar{v}}}-e^{-j\omega\frac{|x_i-\overline{x_{(t)}}|}{\bar{v}}}}S_{i(\omega;t)} \quad (12)$$

Here, $s_{i(t)}$ is compensated by using this inverse filter, and we can obtain the compensated EMG signal $c_{i(t)}$, which is independent of the movement of the innervation zone.

Of note is that the transfer function of (12) has a pole at

$$|x_{i-1}-\overline{x_{(t)}}|=|x_i-\overline{x_{(t)}}|=\frac{\delta}{2} \quad (13)$$

and (12) is unstable near the pole. If $s_{i(t)}$ is not equal to 0, $c_{i(t)}$ will have a large value. In order that $c_{i(t)}$ does not approach infinity, the 20th-order Bessel band-pass filter of 5 to 400 Hz is applied to the compensated signals.

3. Experimental Procedure

Five healthy human subjects (subj. 1 to 5) were recruited and the surface EMG signals of their brachial biceps and their elbow joint angles were measured simultaneously. The experimental setup is shown in Fig. 4. A subject was asked to sit down in front of a flat table and to put his right forearm on the table. Then he was to bend his forearm horizontally from 0 rad to $\pi/2$ rad and to slide a constant load of 3 kg on the table. The surface EMG signals of the brachial biceps were measured by six pairs of Ag-AgCl surface electrodes (5 mm diameter) and bio-amplifiers (Fukuda Denshi, MIC-9800), and the elbow joint angle $\theta_{(t)}$ was also measured simultaneously by a hand-made potentiometer.

The surface electrodes were located to cover the movement range of the innervation zone as shown in Fig. 5. In this figure, the innervation zones of subj. 1 were measured in advance using Masuda and Sadoyama's method [6]. The electrode diameter was 5 mm and δ was 1 cm. The point x_3 was located at the middle of the movement range of the innervation zone and defined as

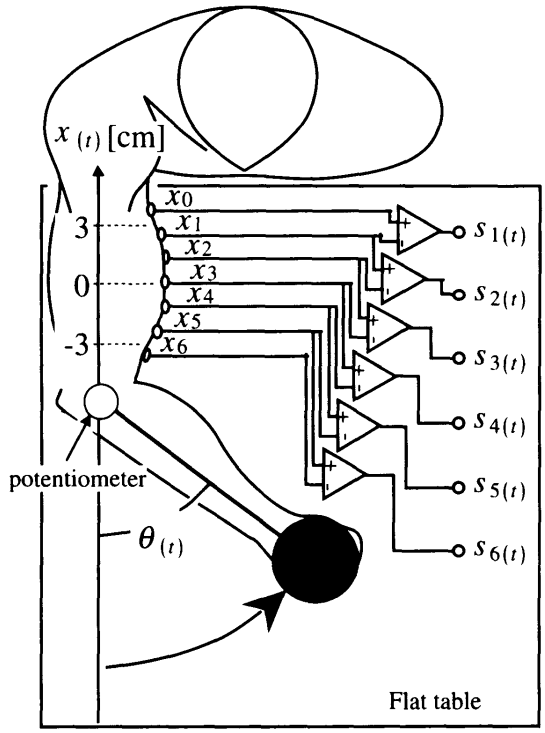

Fig. 4 Experimental procedure. Subject bends forearm on a horizontally flat table with a constant load of 3 kg held by the hand. Surface EMG signals of the brachial biceps were measured from six pairs of Ag-AgCl surface electrodes (5 mm diameter). The parameters are as follows. δ =1 cm, x_6 =–3.0 cm, x_5 =–2.0 cm, ..., and x_0 = 3.0 cm.

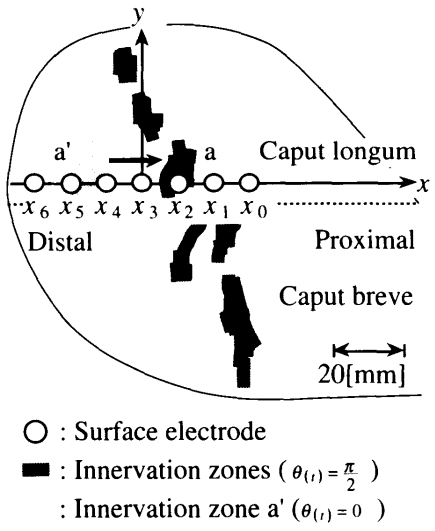

Fig. 5 Distribution of innervation zones and the location of the surface electrodes on the brachial biceps. The innervation zones were measured using Masuda and Sadoyama's method, where the muscle contraction strength was 50 % of the maximum voluntary contraction, the multichannel pin electrodes were in a 9x16 matrix, and the distance between pin electrodes was 2.54 mm. The innervation zone across the electrode line moves from point a' to point a when the subject's arm bends.

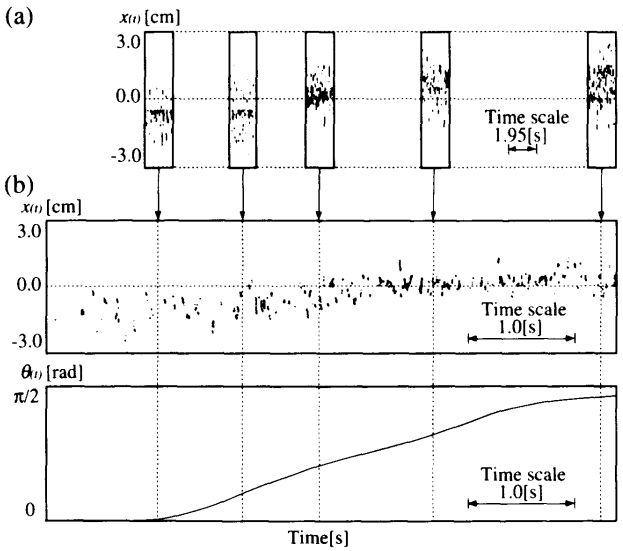

Fig. 6 Estimated $x_{(t)}$, where M = 9, τ = 4 ms, $\bar{v}$ = 4.5m/s , and γ = 1m/s . The plots (a) and (b) indicate the results when our estimation method is applied to static contractions and a dynamic contraction, respectively. The estimated $x_{(t)}$ is displayed against the time course of $\theta_{(t)}$.

x_3 =0 cm, and x_6 and x_0 were placed at –3.0 cm and 3.0 cm from x_3, respectively.

The EMG signals were filtered by the 20th-order Bessel band-pass filter of 5 to 400 Hz, and digitized with a 12-bit analog-to-digital converter (Canopus, ADX-98E) at a sampling rate of 5 kHz. Data acquisition was performed by a personal computer (EPSON, PC-286VF), and data processing was achieved by a workstation (Hewlett-Packard, Apollo9000-720/CRX).

4. Results

4.1 Estimation of an Innervation Zone

Figure 6 shows the results of estimating $x_{(t)}$ for subj. 1, where M was 9, and τ was 4 ms in the NOM filter. Moreover, the appropriate range of $v_{(t)}$ is limited from 4.0 to 5.0 m/s (i.e., $\bar{v}$ = 4.5m/s and γ = 1m/s; here $\bar{v}$ and γ are determined by the time delay between two channels far from the the innervation zones and the error range of it).

Figures 6(a) and (b) indicate the results of applying our estimation method to static contractions and a dynamic contraction, respectively. In these figures, the estimated values of $x_{(t)}$ are displayed against the time course of $\theta_{(t)}$. Here, we can see that the larger the elbow angle becomes, the more $x_{(t)}$ increases. Comparing Fig. 6 with Fig. 5, the values of $x_{(t)}$ estimated by our method are similar to the movement range measured using Masuda and Sadoyama's method.

Moreover, this method was applied to four other subjects during rapid contractions (i.e., bending the arm from $\theta_{(t)}$ =0 to π/2 rad in approximately 1.7 s). As a result,

the synchronous movement of $x_{(t)}$ with $\theta_{(t)}$ was observed in three of the four subjects.

4.2 Compensation for Distorted EMG Signals

Figures 7(a) and (b) show the EMG signals employed in Fig. 6(b). $x_{(t)}$ and $\overline{x_{(t)}}$ were plotted as dots and a line in Fig. 7, respectively. Here, $\overline{x_{(t)}}$ was obtained as the time-local mean value of $x_{(t)}$ before and after 50 ms. The value of $\overline{x_{(t)}}$ was under the 4th electrode pair and the 3rd electrode pair in Figs. 7(a) and (b), respectively. Almost all of the waveforms derived from the electrode pairs were similar to each other; however, $c_{4(t)}$ in Fig. 7(a) and $c_{3(t)}$ in Fig. 7(b) were larger than those of other channels when $\overline{x_{(t)}}$ was between the detecting electrode pair. The causes of this effect, namely, overcompensation, will be discussed in the following section.

Figure 8 shows the variation in the gain characteristics of $H_{3(\omega;t)}$ with time in relation to the movement of the innervation zone $\overline{x_{(t)}}$ during the compensation procedure of $s_{3(t)}$ shown in Fig. 7. Figures 8(a), (b) and (c) show $\overline{x_{(t)}}$, $D_{3(t)}$, and the related time-dependent gain characteristics of $H_{3(\omega;t)}$, respectively. Comparing the former and latter parts of the exercise, there is a more pronounced high-pass filter effect in the latter part of the exercise; i.e., the innervation zone existed between x_2 and x_3, when $D_{3(t)} <$ δ = 1 cm.

5. Discussion

5.1 Validity of the Propagation Model

In this study, many assumptions were made to simplify the propagating behavior of action potentials and to construct our model. The first key assumption was that the endplates of a motor unit are not distributed over a wide range. It was also assumed that only one motor unit action potential was generated at any given time. Moreover, assuming that concepts such as double conduction, decrementless conduction, isolated conduction, and constant conduction velocity of myofibers are applicable, we considered the distribution of the action potentials on the skin surface to be absolutely symmetrical with respect to the center of the innervation zone.

However, multiple innervation zones are sometimes present in skeletal muscle, the endplates are randomly distributed in innervation zones, and a surface electrode detects the action potentials of many myofibers from many motor units. Thus, the influence of the movement of innervation zones on the surface EMG signals is complex and the propagation model is not completely correct. For example, when different innervation zones in a muscle are

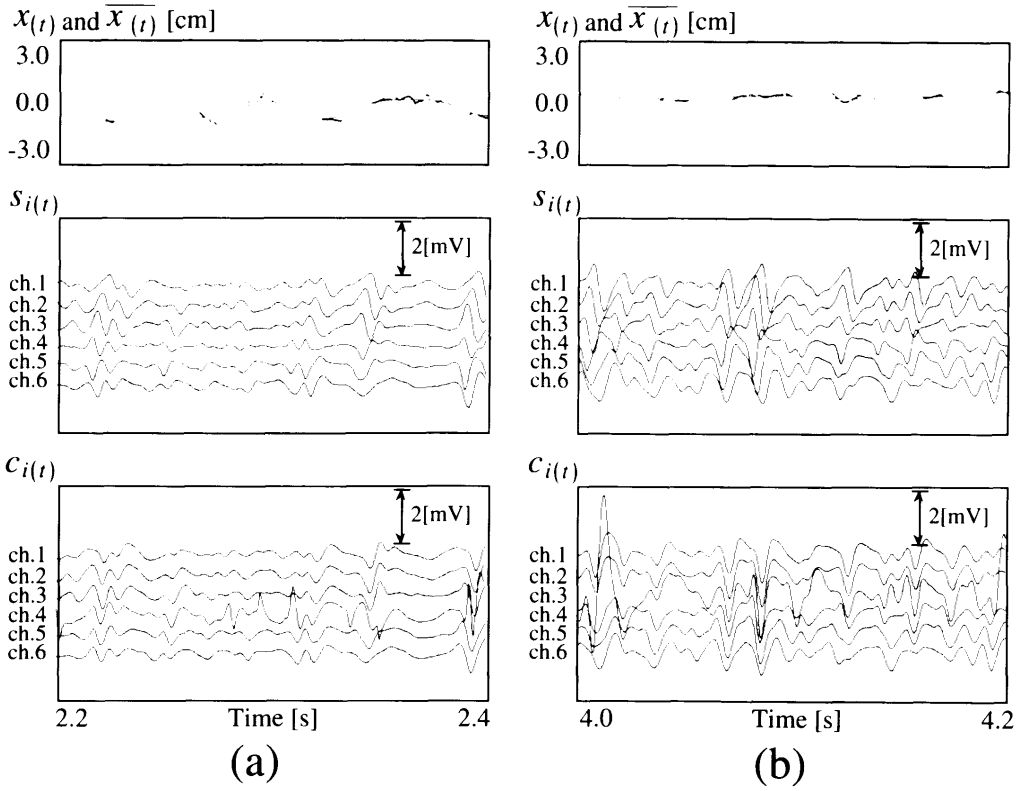

Fig. 7 Compensation results. The dotted plots of $x_{(t)}$ were the estimated positions of an innervation zone and the solid line of $\overline{x_{(t)}}$ is the time-local mean value of $x_{(t)}$. In (a) (i.e., during 2.2 to 2.4 s), $\overline{x_{(t)}}$ was positioned under the 4th electrode pair. In (b) (i.e., 4.0 to 4.2 s), $\overline{x_{(t)}}$ was positioned under the 3rd electrode pair. After the compensation, almost all of the waveforms were similar to each other. However, $c_{4(t)}$ in (a) and $c_{3(t)}$ in (b) are larger than those of the other channels because of overcompensation by inverse filtering.

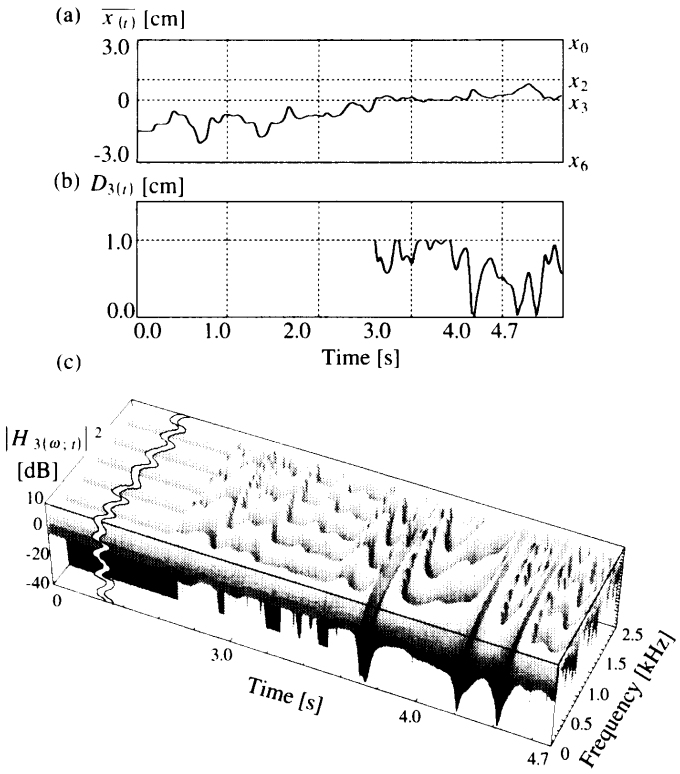

Fig. 8 Variation of $|H_{3(\omega;t)}|$ during the compensation procedure of $s_{3(t)}$. The plots (a), (b), and (c) show $\overline{x_{(t)}}$, $D_{3(t)}$, and the related time-dependent $|H_{3(\omega;t)}|$, respectively. When $\overline{x_{(t)}}$ was between x_2 and x_3 during the latter part of the exercise, $D_{3(t)}$ was less than δ = 1 cm and $|H_{3(\omega;t)}|$ was variable.

activated simultaneously, the EMG signal on the distal side is different from that on the proximal side, even when the phase shift of the EMG signal is considered. Furthermore, the same phenomenon occurs in different endplates in an innervation zone. In those cases, the distribution of the action potentials is unsymmetrical and the correlation between two different EMG signals decreases.

In the present experiments, we made the muscle contraction weak and reduced the possibility of producing two or more action potentials at the same time. Under these conditions, we confirmed experimentally that the action potentials on the skin surface were distributed almost symmetrically. Furthermore, in four of the five subjects tested, the method confirmed that the estimated value of $x_{(t)}$ was directly related to $\theta_{(t)}$, which is related to the muscle length. Although the above assumptions are not completely accurate, we believe that the propagation model is generally applicable to the measurement of surface EMG signals, and useful for explaining the consequences of the effects of the movement of the innervation zone or for validating the processing techniques of EMG signals.

5.2 Accuracy of the Estimation Method

The position of an innervation zone was estimated by using the relationships among the observation positions of the EMG signals, the transition time of action potentials, and the conduction velocity of action potentials. To simultaneously solve the equations constructed by (9a), (9b) and (9c), the transition time of action potentials and the observation positions of the EMG signals should be determined in advance. The transition time of action potentials is calculated from the time delay between each pair of EMG signals, and the observation positions of the EMG signals are determined from the known location of the electrodes. Thus, the reliability of the results suffers from the accuracy of the estimated transition time of action potentials. In the following, the parameters that caused errors in the estimated transition time are discussed.

1) Smoothing effect caused by the surface electrodes and the volume conductor under the skin: Using the estimation method, the movement of the innervation zone has been confirmed in four of the five subjects. However, the method was not applicable to one subject because his observed EMG waveforms were too smooth and the correlation value between each pair of EMG signals was markedly lower than those of other subjects. Using an O fat meter, his hypodermic fat (11 mm) was found to be thicker than those of other subjects (4-6 mm). Thus, the smoothing effect on each electrode surface and the tissue filter [1] which acts as a volume conductor under the skin can account for the above results.

To measure the conduction velocity of the action potentials more accurately, the smoothing effect along the myofibers should be small. Namely, the width of the surface electrode along the myofibers should be small and the volume conduction effect should be small. In future studies, if small surface electrodes are employed, $v_{(t)}$ will be more correctly calculated and the reliability of $x_{(t)}$ will increase.

2) Sampling frequency: To derive the conduction velocity of action potentials, the time delay from each pair of EMG signals was calculated using the correlation method. Usually the calculation of the correlation value is accomplished in discrete time by sampling the waveforms. Since this method only allows discrete time shifts, the temporal resolution is only 0.5 sampling interval, and a high sampling rate is necessary to achieve sufficient resolution for accurate calculation. For example, assuming the conduction velocity of action potentials is 5 m/s and the distance between the channels is 1 cm, the transition time from one channel to an adjacent channel is 2 ms. In the discrete-time process used in this study, the accuracy of the time delay calculation is 0.2 ms because the sampling frequency is 5 kHz. If time delay is overestimated by 0.2 ms, the estimated conduction velocity is reduced to about 4.54 m/s, which leads to an error of 0.46 m/s. Since the conduction velocity varies typically from 3 m/s to 7 m/s[8]-[10], an error of this magnitude is a serious issue. Here, to reduce the magnitude of error, the conduction velocity is limited by the acceptable range of the conduction velocity, γ =1 m/s, and the estimated values of $x_{(t)}$ and $v_{(t)}$ were tested. In future studies, a higher sampling frequency must be used.

3) Number of channels (N) and electrode intervals (δ): To solve the simultaneous equations of (9), one of the equations should be of the form of (9a), which includes both $x(t)$ and $v(t)$. This means that one or more channels should straddle both the distal side and the proximal side relative to the innervation zone. On the other hand, to obtain (9b) or (9c), two or more channels should be on either the distal side or the proximal side of the innervation zone. Considering this, N should be 4 or more, and we must determine N and δ so that the surface electrodes cover the range of movement of the innervation zone. In practice, the noise effect associated with EMG signals must also be taken into account. Thus, N was set large enough (i.e., N =6, δ =1 cm) to avoid these potential problems. In clinical use, e.g., a prosthesis controlled by EMG signals, however, N should be as small as possible. Consequently, further studies are required to determine the suitable value of N and the optimum value of δ.

4) Time constant τ and order M of the NOM filter: Using the NOM filter, we can extend the EMG signal to a polynomial function. The vector that is constructed by the extension coefficients indicates the running spectrum of the EMG signal. Because the vector is not directly related to time t, it can easily be regarded as an instantaneous vector. Thus, the NOM filter is appropriate for the analysis of EMG signals during dynamic contractions.

In the NOM filter, the time constant τ is the time period in which the EMG signal is stationary. Furthermore, the order M is also determined so that the amplitude of $s_{i,M}(t)$ is equal to the noise level. Namely, τ and M are determined by the dynamics of the EMG signal and noise level, respectively.

Considering τ and M, we can discuss the limitations of our method in relation to the velocity of movement of the innervation zone. In the NOM filter, it is assumed that the EMG signal is stable at time τ. Thus, the innervation zone must be between the same electrode pair for the duration of τ. That is, the velocity of movement of the innervation zone must be lower than δ =1 cm during the time τ =4 ms (i.e., 2.5 m/s). For the exercise used in this study, the movement of the innervation zone was estimated to be 0.012 m/s, which is less than this critical value (i.e., about $\theta(t) = 0$ to $\pi/2$ rad per 1.7 s). For faster movement, the noise caused by the mechanical vibration of the surface electrodes does not allow accurate estimation of the movement of the innervation zone. If this noise can be suppressed in future studies, then our method will be applicable to the measurement of faster movement.

5.3 Accuracy of the Compensated EMG Signals

Most of the compensated EMG signals in Fig. 7 have almost the same waveform. However, the waveforms of the 4th channel in Fig. 7(a) and the 3rd channel in Fig. 7(b) were dissimilar with those of the other channels. Since their amplitudes are larger than those of the other channels, the overcompensation phenomenon must have occurred during the compensation by (12). If (13) is satisfied, $s_i(t)$ must be 0 and $c_i(t)$ must also be 0. However, $s_i(t)$ is practically not equal to 0 because of the estimation error of $\overline{x(t)}$, the scattering of the endplates, and the background noise. Since the denominator of (12) is too small, the value of $s_i(t)$ becomes extremely large. Consequently, the overall accuracy of the method relies on how accurately $x(t)$ and $\overline{x(t)}$ can be estimated in advance.

In future studies, new methods to continuously estimate $x(t)$ and $v(t)$ must be developed. Since the method presented here allows us to evaluate the waveforms of motor unit action potentials more accurately and abstract the position of innervation zones, detailed analysis of the bipolar surface EMG signals will be realized.

6. Conclusion

In this study, using the propagation model of the action potentials, we developed a compensation method for the distortion of EMG signals caused by the movement of an innervation zone. Our method is based on the multichannel surface EMG measurement, an instantaneous correlation method, and the inverse filtering technique.

As a result, the movement of the innervation zone could be estimated in four out of the five subjects. We found that the compensated EMG signals have almost the same waveform, except for those of the channels near the innervation zone.

In future studies, to enable detailed analysis of bipolar surface EMG signals, we intend to improve the accuracy of estimating the position of innervation zones and the conduction velocity of action potentials.

Acknowledgment

The authors wish to thank T. Masuda and T. Sadoyama for useful discussion. This research was partially supported by the TEPCO Research Foundation.

References

[1] L.H.Lindström and R.I.Magnusson, "Interpretation of myoelectric power spectra: a model and its applications," Proc. IEEE, vol.65, pp.653-662, 1977.
[2] H.Reucher, J.Silny, and G.Rau, "Spatial filtering of noninvasive multielectrode EMG: part II - filter performance in theory and modeling," IEEE Trans. Biomed. Eng., vol.BME-34, pp.106-113, 1987.
[3] T.Masuda and T.Sadoyama, "Distribution of innervation zones in the human biceps brachii," J. Electromyography and Kinesiology, vol.1, pp.107-115, 1991.
[4] S.H.Roy, C.J.De Luca, and J.Schneider, "Effects of electrode location on myoelectric conduction velocity and median frequency estimates," J. Appl. Physiol., vol.61, pp.1510-1517, 1986.
[5] G.F.Inbar, J.Allin, and H.Kranz, "Surface EMG spectral changes with muscle length," Med. & Biol. Eng. & Comput., vol.25, pp.683-689, 1987.
[6] T.Masuda and T.Sadoyama, "Topographical map of innervation zones within single motor units measured with a

grid surface electrode," IEEE Trans. Biomed. Eng., vol.35, no.8, pp.623-628, 1988

[7] T.Iijima, "Fundamental theory of wave form analysis based on natural observation method," IEICE Trans., vol.J68-A, no.3, pp.302-308, 1985.

[8] T.Sadoyama and T.Masuda, "Changes of the average muscle fiber conduction velocity during a varying force contraction," Electroencepharography and Clinical Neurophysiology, vol.67, pp.495-497, 1987.

[9] M.Naeije and H.Zorn, "Estimation of the action potential conduction velocity in human skeletal muscle using the surface EMG cross-correlation technique," Electromyogr. Clin. Neurophysiol., vol.23, pp.73-80, 1983.

[10] H.Nishizono, H.Kurata, and M.Miyashita, "Muscle fiber conduction velocity related to stimulation rate," Electroencephalography and Clinical Neurophysiology, vol.72, pp.529-534, 1989.

Hidekazu Kaneko was born in Niigata, Japan, on November 22, 1964. He received the B. S. and M. S. degrees in information engineering in 1987 and 1989, and the Ph. D. degree in biosignalling in 1992, all from Niigata University, Niigata, Japan. In 1992 he joined the Industrial Products Research Institute, AIST, MITI, Japan, as a researcher. From 1993 he is belonging in the National Institute of Bioscience and Human-technology, AIST, MITI, Japan. He works in the areas of biosignalling in medical fields. He is currently interested in the interpretation of plural neuronal activities. He is a member of IEEE-EMBS.

Tohru Kiryu was born in Niigata Prefecture, Japan, in 1952. He received the B. E. and M. E. degrees in electronics engineering from Niigata University, Niigata, Japan, in 1975 and 1977, respectively and the Dr. Eng. degree in computer science from Tokyo Institute of Technology, Tokyo, Japan, in 1985. From 1977 to 1978, he was an Assistant at the school of dentistry of Niigata University. From 1978 to 1995, he was with the Department of Information Engineering, Niigata University. Since 1995, he has been with the Graduate School of Science and Technology, Niigata University as a Professor. From June 1990 to March 1991, he studied at the Neuro Muscular Research Center at Boston University as a Visiting Scientist. He has been working on biomedical signal processing, especially time-varying spectral analysis, time-varying parameters estimation using nonstationary models and nonstationary stochastic process. For applications, his recent interests have been in myoelectric signal analysis during dynamic movements, muscular fatigue evaluation at a required time, and mental stress evaluation from multidimensional time-series. Dr. Kiryu is a member of the Institute of Electrical and Electronics Engineers, the Japan Society of Medical Electronics and Biological Engineering and the Japan Prosthodontic Society.

Yoshiaki Saitoh was born in Niigata Prefecture, Japan. He received the B. E. degree in electrical engineering from Niigata University, Niigata, Japan, in 1963, and the M. E. and Ph. D. degrees in electrical engineering from Hokkaido University, Sapporo, Japan, in 1965 and 1970, respectively. In 1965, he joined the staff of the Department of Electronics, Niigata University, as an Instructor. Since 1980, he has been a Professor in the Department of Information Engineering at Niigata University. His recent research interests include measurements and stimulation of the human organs, hyperthermia systems, electrocardiogram data compression, and other biomedical signal processing. Dr. Saitoh is a member of the Institute of Electrical and Electronics Engineers, the Japan Society of Medical Electronics and Biological Engineering.